International Journal of ChemTech Research
CODEN (USA): IJCRGG, ISSN: 0974-4290, ISSN(Online):2455-9555
Vol.10 No.2, pp 948-960, 2017

Investigations on effect of FCAW process variables in heat loss reduction clad layers

M.Sowrirajan[1]*, P.Koshy Mathews[2], S.Vijayan[1], D.Saravanan[1], R.Renugadevi[1]

[1]Department of Mechanical Engineering, Coimbatore Institute of Engineering and Technology, Tamil Nadu, India
[2]Department of Mechanical Engineering, Kalaivani College of Technology, Tamil Nadu, India

Abstract : Weld cladding is a process of depositing a material over another material by a suitable welding process to enhance various surface properties of a material. This work deals with the metal cladding process to conserve a quantity of heat energy in pressure vessels. It is done by producing a low thermal conductivity material layer over a high thermal conductivity boiler material plate. Austenitic stainless steel grade 316L is deposited over IS: 2062 structural steel plates using FCAW process. Five factors five levels rotatable central composite design is used for experimentation. Experimental study is carried out on shape relationship factors and capable mathematical models are developed for the prediction. Direct and interaction effects of process parameters on surface shape quality characteristic factors are discussed.
Key words : Cladding, heat loss, thermal conductivity, Response surface methodology.

Introduction

Metal cladding is a technique developed especially to enhance chemical, mechanical and metallurgical properties of material surfaces. Numerous fields viz. chemical plants, fertilizer plants, nuclear power plants, pressure vessels, agricultural machines, railways and even aircraft and missile components are started making use of this technique to enhance the properties and/or repair of the worn out components at their surfaces with feasible cost instead of replacing them completely [1]. Shielded metal arc welding, submerged arc welding, gas tungsten arc welding, metal inert gas welding, electron beam welding, explosive welding and laser welding are some important welding processes involved in clad surfacing [2-8]. Effective selection and control of welding process parameters are very much essential in producing quality claddings[9]. Quality of cladding is assessed based on bead geometry. Basic clad bead geometry includes reinforcement or bead height, bead width and depth of penetration [3]. Fig. 1 shows the basic bead geometry factors of a cladding process. Reinforcement form factor and penetration shape factor are the shape relationship factors relating basic bead geometry dimensions[3]. These factors are believed to speak about the surface quality of the cladding since they are concerning about the external and internal shape of the clad beads respectively. In multipass cladding, melting capability of first layer, effect of dilution and range of heat affected zone (HAZ) are decided by these shape factors[2].Hence, study of these factors is important in the field of clad surfacing.

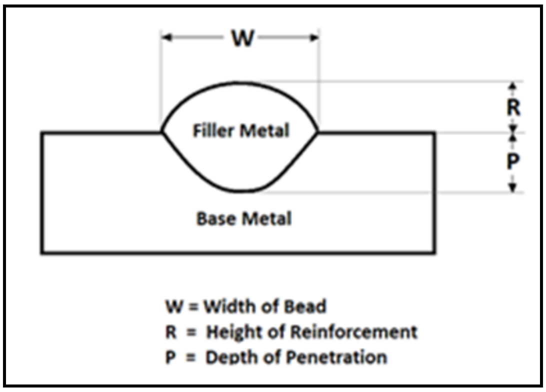

Fig. 1 Basic bead geometry

Conduction heat transfer is the transfer of heat energy through the molecules of a solid medium due to temperature gradient [10]. In the expression for calculating the conduction heat transfer across a composite layer ($Q=\Delta T/R$), heat transfer is indirectly proportional to resistance (R). However, as $R=L/kA$, resistance is directly proportional to the thickness of the material (L_1& L_2) and indirectly proportional to the thermal conductivity of the material layers (k_1& k_2)[11,12]. Reduction in heat loss is possible if the clad layer is formed using low thermal conductivity material as shown in Fig. 2. Especially, Heat loss is possibly reduced with increase in clad bead height as it helps to increase the clad layer thickness. Temperature drop across a composite layer is depends on thermal conductivity (k_1& k_2) of layer materials and thermal contact resistance at the interface. Fig. 2 shows the concept of temperature drop across the composite layers made by cladding process. Usually composite clad layer sections are formed in pressure vessels to improve surface properties of base material[3,11]. Regularly, a definite quantity of heat energy is continuously transferred to the atmosphere through the walls of the pressure vessels. Reducing this conduction heat loss up to a possible extend helps the equipments to increase the efficiency up to a considerable level. Hence it is important to study the ways to reduce the heat loss.

As clad bead shape is indicated by reinforcement form factor and penetration shape factor, these factors could control the shape of clad layer and contact resistance. Hence this work aims to produce the clad layer for reducing heat loss and to analyze the effect of welding process parameters on clad quality parameters. In this paper, reinforcement form factor and weld penetration shape factor were chosen as responses to evaluate the surface quality of 316L stainless steel clad deposits on structural steel by FCAW process. The experiments were conducted based on central composite design and the output factors were calculated after measuring bead dimensions. The mathematical models were developed for the responses. Direct and interaction effects of process variables on the responses were presented in graphical form and discussed elaborately.

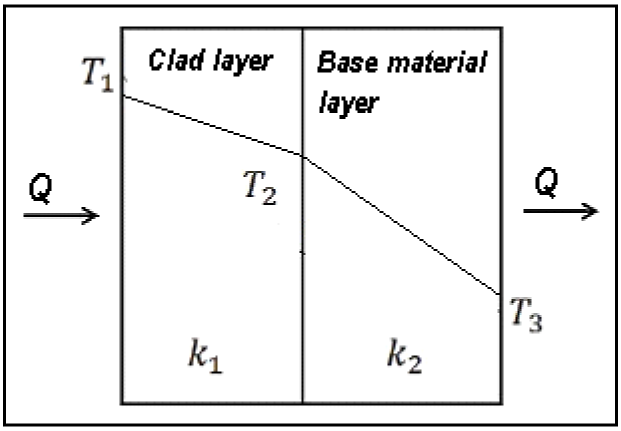

Fig. 2 Concept of temperature drop across a composite layer

Experimental work

Structural steel (ASTM A 105 / IS: 2062) was selected as the base material, since it is used widely in applications like pressure vessels, automotive industries, high temperature applications etc. The structural steel plates of dimensions 100x50x20 mm were prepared to carry out this study. Austenitic stainless steel, 316L flux cored filler wire of 1.2 mm diameter was used pursue this research work. Open circuit voltage (V), wire feed rate (F), welding speed (S), nozzle to plate distance (D) and electrode angle (E) were selected and lower and upper limits of each variable were found by conducting trial runs. The intermediate values were arrived to meet the number of levels by using suitable formula[13]. The details of the process parameters are given in Table 1.

Table 1 Details of FCAW process parameters

Parameters (Coded)	**Units**	**Levels**				
		-2	**-1**	**0**	**+1**	**+2**
Voltage (V)	Volts	30	32	34	36	38
Wire feed Rate (F)	m/min	9	11	13	15	17
Welding speed (S)	m/min	0.18	0.26	0.34	0.42	0.5
Nozzle to plate distance (D)	mm	17	19	21	23	25
Electrode angle (E)	degree	5	10	15	20	25

The prepared structural steel plates were pre-processed using grinding and cleaning operations to facilitate metal joining[14]. Esseti-Unimacro 501C welding machine was used to perform weld cladding on all 32 plates. 40% overlapping was maintained to lay three beads on each plate in order to maintain an optimum and acceptable dilution[15,16]. A gas mixture of 95% CO_2 and 5% Argon was used as shielding gas and allowed to flow at a constant rate of 18 litres per minute. The specimens were allowed to cool naturally between every passes to reduce heat affected zone (HAZ). Welded plates were then allowed for air cooling, then processed with fine grade of emery papers and etched in 5% nital solution for meeting metallurgical procedures. Few clad specimens are shown in Fig. 3

Fig.3 Few clad specimens during experimental runs

Reinforcement form factor (RFF) and weld penetration shape factor (WPSF) were considered as final output responses. Specimens were cut into cross sections such that so as to ensure the size of 50x50x20 mm for heat transfer experimentation. Measurements were made using profile projector for clad height (R), clad width (W) and depth of penetration (P). Reinforcement form factor and weld penetration shape factor values were calculated using the equations[2], RFF=W/R, WPSF=W/P and presented in the Table 2.

Development of mathematical models and conformity tests

Mathematical models were developed based on the regression coefficients arrived using MINITAB 14 software package as follows. Response function involved to denote the responses could be expressed as Response, Y = f (V, F, S, D, E). The following second order polynomial equation was selected to represent response surface of responses for five variables, in which coefficient b_0 is the constant term; coefficients b_1, b_2,

b_3, b_4 and b_5 are linear terms; coefficients b_{11}, b_{22}, b_{33}, b_{44} and b_{55} are square terms; coefficients b_{12}, b_{13}, b_{14}, b_{15}, b_{23}, b_{24}, b_{25}, b_{34}, b_{35} and b_{45} are interaction terms[13].

$$Y = b_0 + b_1V + b_2F + b_3S + b_4D + b_5E + b_{11}V^2 + b_{22}F^2 + b_{33}S^2 + b_{44}D^2 + b_{55}E^2 + b_{12}VF + b_{13}VS + b_{14}VD + b_{15}VE + b_{23}FS + b_{24}FD + b_{25}FE + b_{34}SD + b_{35}SE + b_{45}DE \quad (1)$$

Table 2 Design matrix with response values

Runs	FCAW process variables (coded)					Response values	
	V (Volts)	**F (m/min)**	**S (m/min)**	**D (mm)**	**E (degree)**	**Reinforcement form factor (RFF)**	**Weld penetration shape factor (WPSF)**
1	-1	-1	-1	-1	1	5.40	41.11
2	1	-1	-1	-1	-1	7.50	46.72
3	-1	1	-1	-1	-1	4.61	27.07
4	1	1	-1	-1	1	7.17	27.50
5	-1	-1	1	-1	-1	7.77	21.98
6	1	-1	1	-1	1	7.46	21.36
7	-1	1	1	-1	1	4.18	20.90
8	1	1	1	-1	-1	4.89	28.78
9	-1	-1	-1	1	-1	3.72	42.40
10	1	-1	-1	1	1	6.51	34.15
11	-1	1	-1	1	1	4.03	50.80
12	1	1	-1	1	-1	6.70	35.00
13	-1	-1	1	1	1	4.14	25.43
14	1	-1	1	1	-1	6.08	37.50
15	-1	1	1	1	-1	3.88	21.56
16	1	1	1	1	1	5.88	19.58
17	-2	0	0	0	0	3.63	24.50
18	2	0	0	0	0	6.93	30.78
19	0	-2	0	0	0	7.14	28.24
20	0	2	0	0	0	4.55	23.36
21	0	0	-2	0	0	6.48	41.18
22	0	0	2	0	0	6.18	16.15
23	0	0	0	-2	0	5.70	18.85
24	0	0	0	2	0	4.60	30.67
25	0	0	0	0	-2	4.79	25.57
26	0	0	0	0	2	5.11	23.00
27	0	0	0	0	0	4.65	25.18
28	0	0	0	0	0	5.47	29.38
29	0	0	0	0	0	5.53	25.32
30	0	0	0	0	0	4.79	22.50
31	0	0	0	0	0	5.24	23.60
32	0	0	0	0	0	5.63	24.20

The values of regression coefficients developed themselves left the clues as to what level the variables affect the responses. Also, the p – values (set as <0.05) were helped to identify the insignificant coefficients, thereby those values were neglected to reduce the complexity in mathematical expressions without disturbing accuracy. F-tests and t-tests were incorporated for achieving this and final mathematical models were developed with the consideration of significant coefficients only [2]. The developed models were involved to test their adequacy by using ANOVA technique. Also, the coefficient of determination (R^2) and adjusted R^2 values were considered as other criterion. As these R^2 values were above an acceptable level of 95%, the developed models are quite adequate[17]. ANOVA table is given in Table 3. Final mathematical models developed with variables in coded as well as uncoded natural form for the responses reinforcement form factor and weld penetration shape factor are given below.

Table 3 Analysis of variance table

Response	Sum of Squares (SS)		Degrees of freedom (DF)		Mean Square value (MS)		F-Value	p-value (Prob> F)	R-Squared (%)	Adjusted R-Squared (%)
	Regression	**Residual**	**Regression**	**Residual**	**Regression**	**Residual**				
RFF	43.4390	1.5413	20	11	2.1720	0.1401	15.50	0.000	96.6	90.3
WPSF	2134.11	109.26	20	11	106.706	9.933	10.74	0.000	95.1	86.3

$$\mathrm{RFF\ (coded)} = 5.21045 + 0.86833V - 0.51667F - 0.42083D + 0.16705F2 + 0.2958S2 - 0.3675VS + 0.275VD + 0.25625VE - 0.37875FS \quad (2)$$

$$\mathrm{WPSF\ (coded)} = 24.3128 - 2.0138F - 6.6946S + 2.3379D + 1.7472V2 + 1.6834S2 + 2.3644VS - 1.8719VD - 4.6194VE + 1.8394FE \quad (3)$$

$$\mathrm{RFF\ (uncoded)} = 5.21045 + 0.434167V - 0.258333F - 0.210417D + 0.0417614F2 + 0.0739489S2 - 0.0918750VS + 0.0687500VD + 0.0640625VE \quad (4)$$

$$\mathrm{WPSF\ (uncoded)} = 24.3128 - 1.00688F - 3.34729S + 1.16896D + 0.436790V2 + 0.420852S2 + 0.591094VS - 0.467969VD - 1.15484VE \quad (5)$$

The validities of regression models were tested by plotting scatter charts. Typical scatter plots are presented in Fig. 4 and Fig. 5 to show the perfection of fit between observed and predicted responses. The scattered chart shows that the both responses are scattered very nearer to 45° straight line, evident a perfect fit for the responses[2]. Also, two experimental runs were performed using different values of process variables other than the values used in the design matrix to evaluate the regression models. The same situation followed during the regular experimental runs was maintained during the conformity test also. The results show good agreement towards the developed models. The results of conformity test experiments are presented in Table 4.

Table 4 Results of conformity experimental runs

V	F	S	D	E	RFF			WPSF		
					Predicted	**Actual**	**% error**	**Predicted**	**Actual**	**% error**
+1	0	2	-1	0	6.67	6.32	-5.2%	23.66	23.00	-2.7%
0	+2	+1	0	+2	4.38	4.21	-3.8%	22.63	22.92	+1.3%

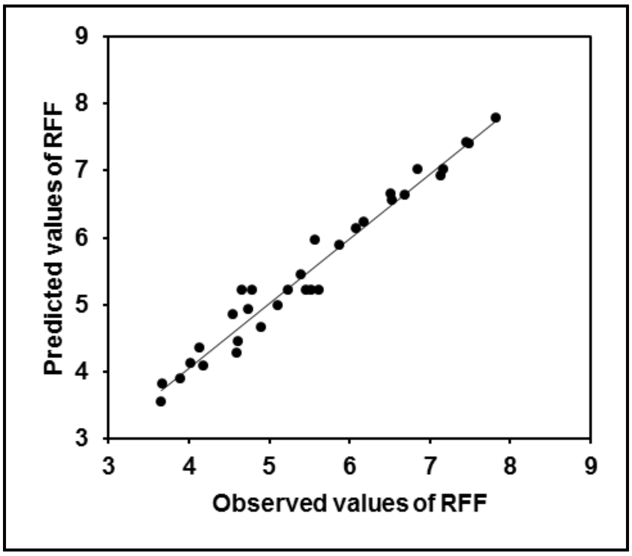

Fig. 4 Scatter chart for RFF

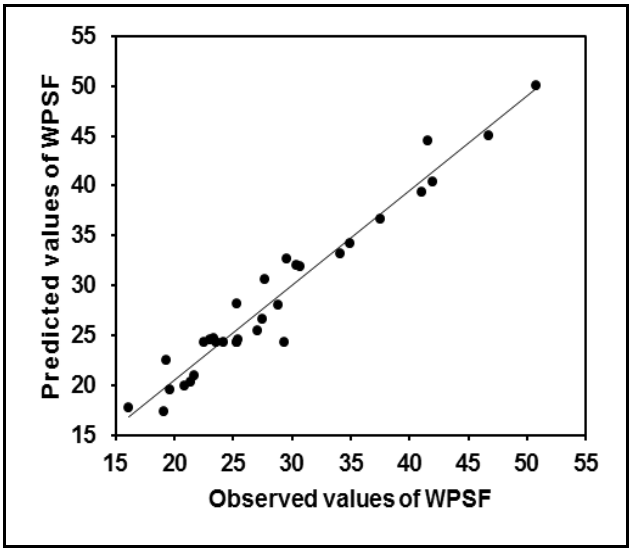

Fig. 5 Scatter chart for WPSF

Results and discussions

The effect of process variables on the responses were evaluated by drawing graphs based on the developed mathematical models in coded forms. The main individual effects and interaction effects of process variables are presented under the subsequent titles.

Direct effects of process variables on reinforcement form factor (RFF) and weld penetration shape factor (WPSF)

It is observed from Fig. 6that RFF increases with increase in open circuit voltage (V). This may be due to increase in the bead width, decrease in bead height with increase in OCV that allow higher deposition rate because of better fluidity of molten wire. Increase in wire feed rate (F) decreases RFF, this may be due to the effect of welding current that increases the deposition of weld metal per unit length of clad bead. RFF initially decreases up to the middle level of welding speed (S) and increases for further increment of S. This effect is attributed to deposition of metal per unit length of plate reduces with increase in welding speed. Increase in nozzle-to-plate distance (D) decreases RFF, may be due to increased arc length over the increase in distance between nozzle and plate (D). It is surprise to note that electrode angle (E) has negligible effect on reinforcement form factor.

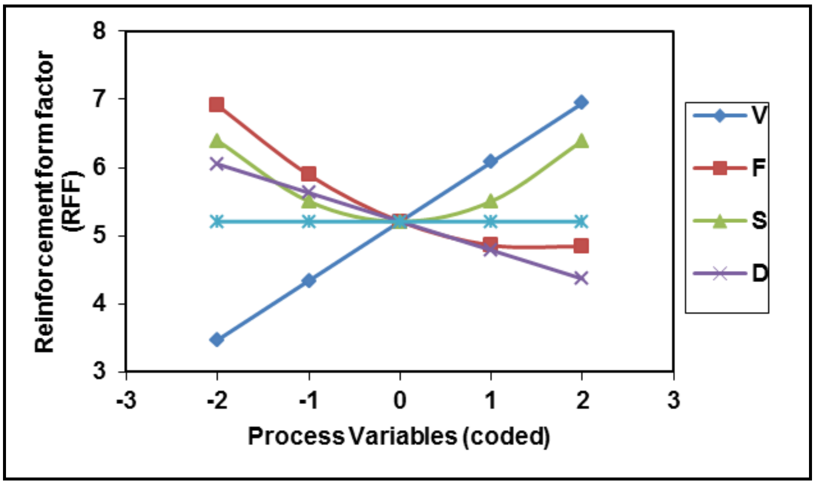

Fig. 6 Main effects of process variables on RFF

Fig. 7 shows that increase in lower values of open circuit voltage (V) decreases WPSF initially and WPSF increases for further increment of V. This is attributed to increased bead width during better fluidity of molten metal wire. Increase in value of wire feed rate (F) decreases the value of WPSF steadily. This may be due to enhanced power input via filler wire causes large volume of metal resulting deep penetration. Welding speed (S) registered its significant influence on WPSF, because its increment decreases WPSF. This is due to the fact that lower welding speed values provides better heat input, hence increased bead width. Further, the increment in welding speed reduces the value of bead width, thereby WPSF. Nozzle-to-plate distance (D) involves in increasing WPSF steadily because of wider bead width due to wider arc cone when D increases. Effect of electrode angle (E) seems insignificant as in the case of RFF. Omission of electrode angle in developed model supports this insignificant reason.

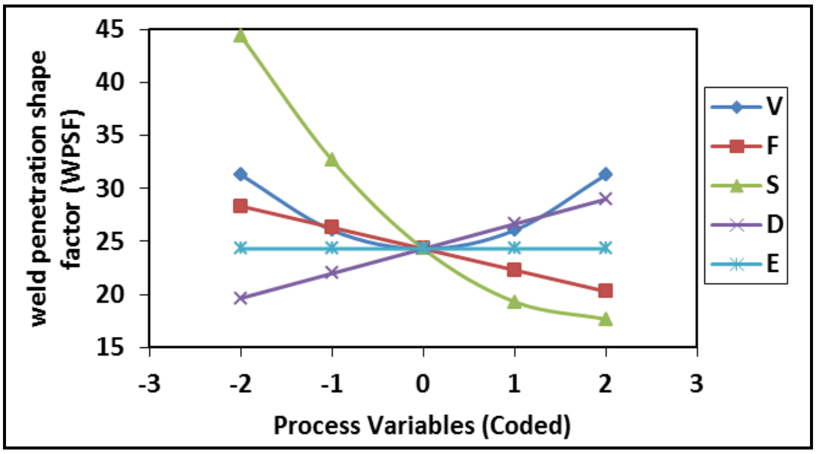

Fig. 7 Main effects of process variables on WPSF

Interaction effects of process variables on reinforcement form factor (RFF) and weld penetration shape factor (WPSF)

Interaction effects of welding process variables are presented in the subsequent headings below. Insignificant change is noted in RFF value from Fig. 8 with the increase in welding speed up to middle level 0 (0.34 m/min) when open circuit value is at its lowest level -2 (30V), but for the further increment of S causes RFF to raise considerably. However, RFF starts decreasing with the increase in values of both welding speed and open circuit voltage collectively. This may be due to the reason that increase in welding speed (S) reduces the bead width and increases the bead height.

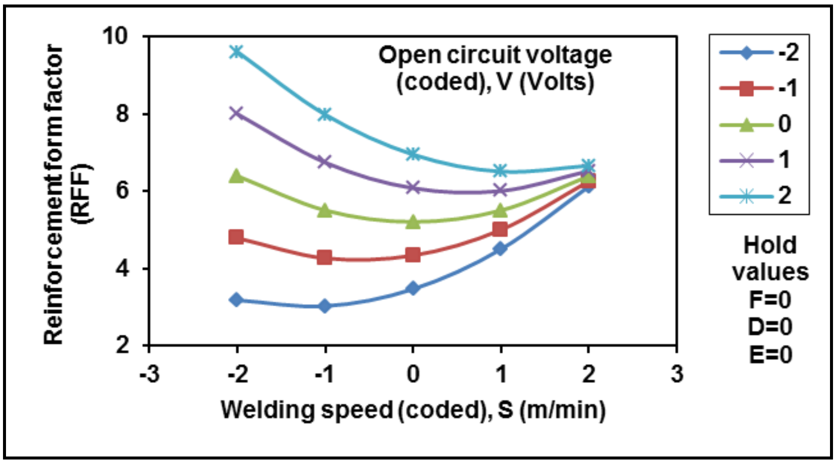

Fig. 8 Interaction effects of open circuit voltage (V) and welding speed (S) on reinforcement form factor (RFF)

Interaction effects of open circuit voltage and nozzle-to-plate distance increases the value of RFF considerably when both open circuit voltage and nozzle-to-plate distance values increases collectively according to Fig. 9. This may be attributed to increase in arc length creates a wider bead width due to spread of arc cone. But RFF remains constant when the value of open circuit voltage is between its levels +1 and +2 (say 37 V) for all the changes in value of nozzle-to-plate distance.

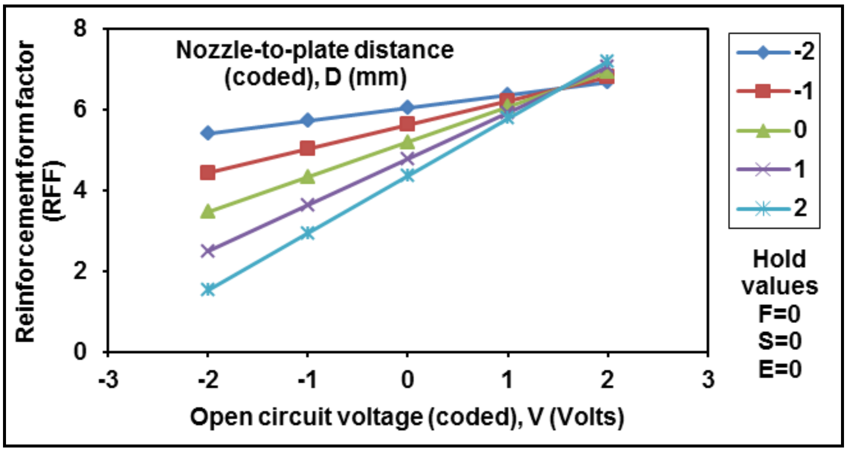

Fig. 9 Interaction effects of open circuit voltage (V) and nozzle to plate distance (D) on reinforcement form factor (RFF)

Fig. 10 shows a rise of RFF with increase in value of open circuit voltage for all levels of electrode angle. However the increment rate of RFF increases significantly when the electrode angle increases from its lower lever to higher level. This may because of the reason that increase in open circuit voltage improves the fluidity of molten metal deposit and thereby increases the bead width. This also may be due to the fact that arc force per arc area scoops the metal pool and results in large bead height at lower values of E. RFF remains unaltered when OCV is at its middle level 0 (34V) for all the levels of electrode angle.

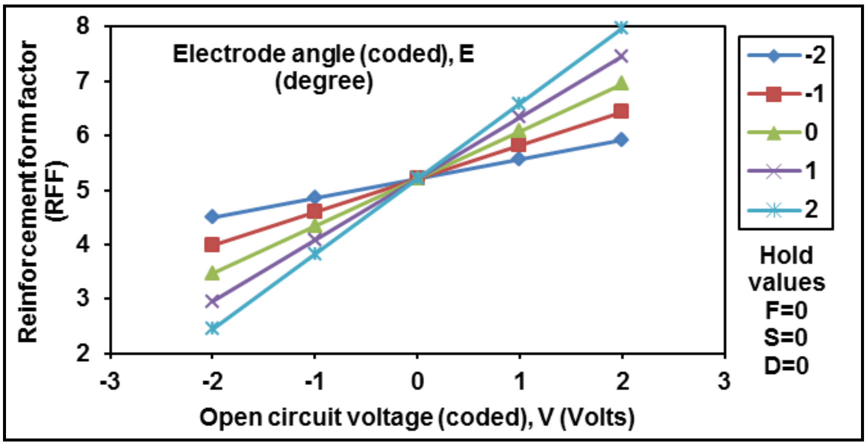

Fig. 10 Interaction effects of open circuit voltage (V) and electrode angle (E) on reinforcement form factor (RFF)

According to Fig. 11, when welding speed increases at lower level of wire feed rate, RFF increases insignificantly. On the other hand RFF decreases radically with increase in welding speed at higher level of wire feed rate. This may be due to the reason that higher welding speed and wire feed rate levels reduces the heat input and registered positive effects on clad height.

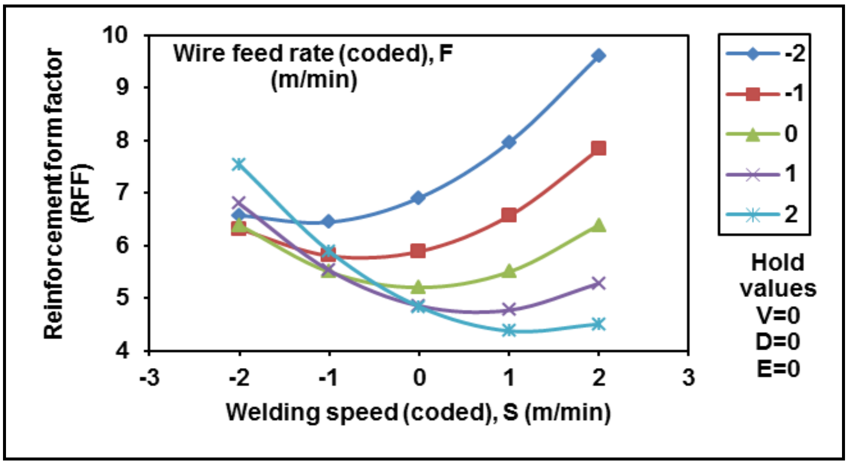

Fig. 11 Interaction effects of wire feed rate (F) and welding speed (S) on reinforcement form factor (RFF)

It is interesting to note from Fig. 12 that RFF decreases radically with increase in wire feed rate at lower level of nozzle-to-plate distance (17mm). But this effect diminishes further with increase in value of nozzle-to-plate distance and followed by a rise in RFF when wire feed rate increases at higher level of nozzle-to-plate distance (25mm). This might be due to increase in arc current and wider arc cone that increases the bead width with enough heat input. RFF looks constant when wire feed rate is at its level +1 (15m/min) for all the levels of nozzle-to-plate distance.

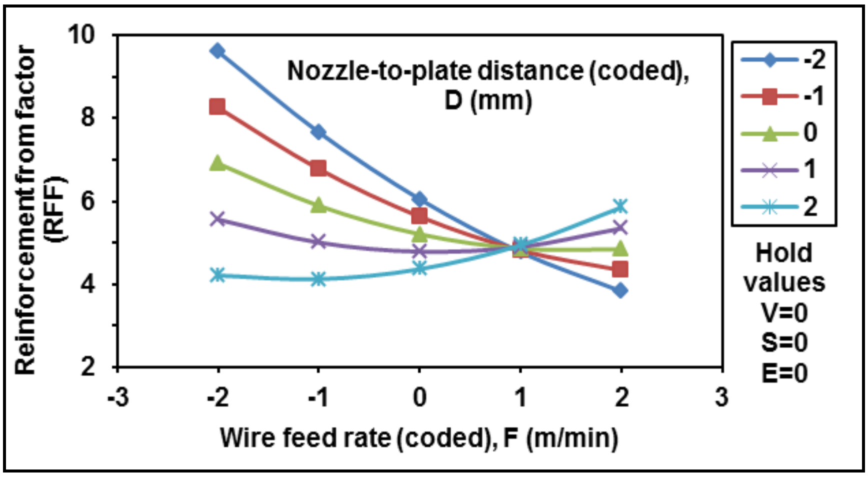

Fig. 12 Interaction effects of wire feed rate (F) and nozzle to plate distance (D) on reinforcement form factor (RFF)

It is to note from Fig. 13 that WPSF decreasing with increase in open circuit voltage at lower level -2 (0.18m/min) of welding speed. On the other hand, WPSF increasing with increase in OCV at higher level +2 (0.5m/min) of welding speed. Increase in welding speed at lower level -2 (30V) of open circuit voltage decreases WPSF radically and increase in welding speed at higher level +2 (38V) of open circuit voltage again decreases WPSF slightly. This may be due the reason that lower welding speed levels helps to extend the focus time duration of heat input on base metal, thus an improved depth of penetration resulting the reduced WPSF.

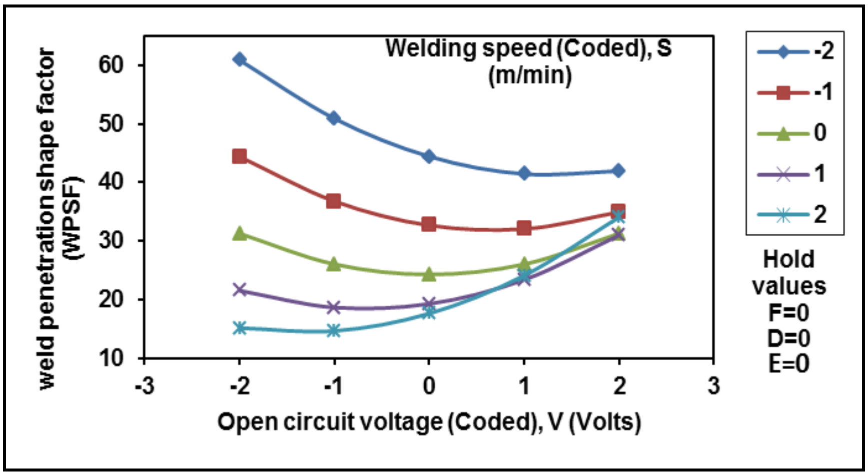

Fig. 13 Interaction effects of open circuit voltage (V) and welding speed (S) on weld penetration shape factor (WPSF)

A considerable fall in the value of WPSF is noted from Fig. 14 when the open circuit voltage increases at the higher level +2 (25mm) of nozzle-to-plate distance. This effect is because of the resistance supplied against the flow of power to the base metal that reduces penetration and improves the bead height rather than bead width. Also, higher level +2 (38V) of OCV at higher level +2 (25mm) of nozzle-to-plate distance turns the WPSF to increase. This is attributed to the reason of improved bead width due to wider arc cone at higher OCV.

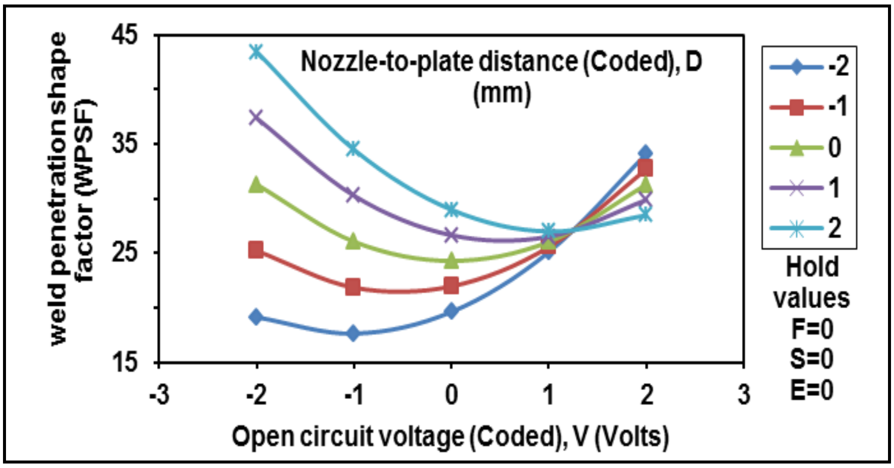

Fig. 14 Interaction effects of open circuit voltage (V) and nozzle-to-plate distance (D) on weld penetration shape factor (WPSF)

Fig.15 shows that significant increase and significant decrease in WPSF observed when open circuit voltage increases at lower and higher level of electrode angle respectively. This is because of the reason that arc force per arc area scoops the metal pool resulting in decrease in bead height and increase in bead width at lower values of electrode angle. However, WPSF remains constant when OCV is at its middle level 0 (34V) for all the levels of electrode angle.

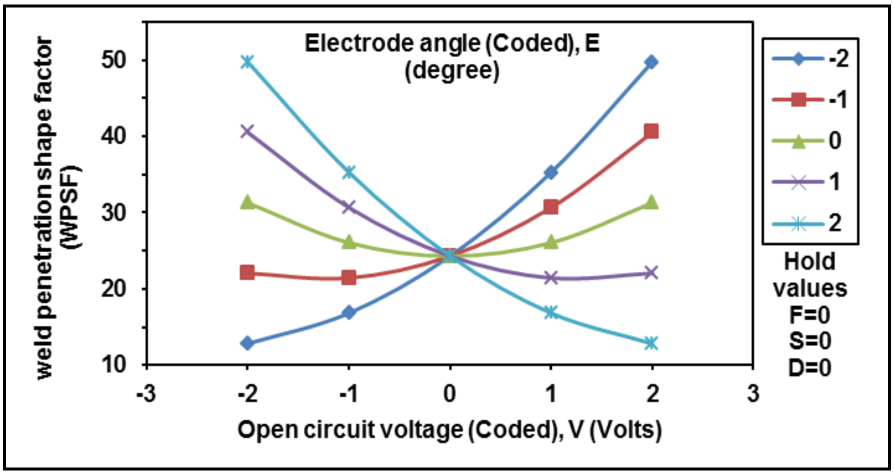

Fig. 15 Interaction effects of open circuit voltage (V) and electrode angle (E) on weld penetration shape factor (WPSF)

It is seen from Fig. 16 that considerable fall and rise in WPSF noted when electrode angle increases at lower and higher level of wire feed rate respectively. However, WPSF remains constant when electrode angle is at its level +1 (20degree) for all the levels of wire feed rate.

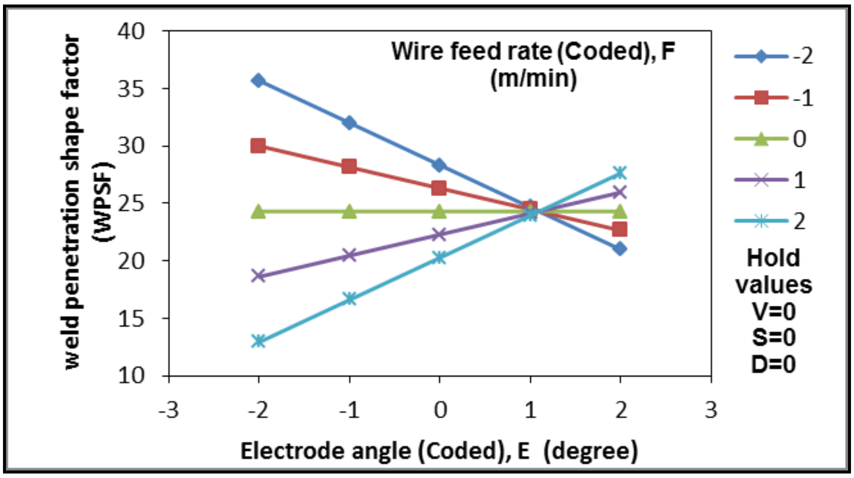

Fig. 16 Interaction effects of electrode angle (E) and wire feed rate (F) on weld penetration shape factor (WPSF)

Conclusions

Response surface methodology was successfully used to analyze and to establish regression models for the prediction of shape of heat loss reduction layers. Conformity tests confirm the prediction capability of models developed for reinforcement form factor and penetration shape factor. Open circuit voltage was the most influencing parameter while wire feed rate, nozzle-to-plate distance and welding speed also were found with considerable effects on reinforcement form factor. Welding speed has great influence in deciding penetration shape factor along with tiny effects from wire feed rate and nozzle-to-plate distance. Electrode angle was the less influencing parameter on both responses comparing other parameters within the values used. Significant interactions were noted between process parameters. Hence, clad quality would not be commendable without considering the effects of interaction between process parameters.

Acknowledgement

Authors wish to thank Faculty of Mechanical Engineering, Coimbatore Institute of Engineering and Technology and Kalaivani College of Technology, Coimbatore, India for providing required facilities and supports to carry out research.

References

1. Murugan N, Parmar RS. Effects of MIG process parameters on the geometry of the bead in the automatic surfacing of stainless steel. Journal of Materials Processing Technology, 1994, 41(4): 381-98.
2. Palani PK, Murugan N. Optimization of weld bead geometry for stainless steel claddings deposited by FCAW, Journal of Materials Processing Technology. 2007, 190(1):291-9.
3. Kannan T, Yoganandh J. Effect of process parameters on clad bead geometry and its shape relationships of stainless steel claddings deposited by GMAW. The International Journal of Advanced Manufacturing Technology, 2010, 47(9-12):1083-95.
4. Palani PK, Murugan N. Development of mathematical models for prediction of weld bead geometry in cladding by flux cored arc welding. The International Journal of Advanced Manufacturing Technology, 2006, 30(7-8):669-76.
5. Kannan T, Murugan N. Sensitivity analysis of flux cored arc cladding parameters using response surface methodology. Journal for Manufacturing Science and Production, 2006, 7(3-4):171-86.
6. Palani PK, Murugan N. Ferrite number optimisation for stainless steel cladding by FCAW using Taguchi technique. International Journal of Materials and Product Technology, 2008, 33(4):404-20.
7. Senthilkumar B, Kannan T. Effect of flux cored arc welding process parameters on bead geometry in super duplex stainless steel claddings. Measurement, 2015, 62:127-36.

8. Mi G, Xiong L, Wang C, Hu X, Wei Y. A thermal-metallurgical-mechanical model for laser welding Q235 steel, Journal of Materials Processing Technology, 2016, 238:39-48.
9. J.H.F. Gomes, S.C. Costa, A.P. Paiva, and P.P. Balestrassi, Mathematical Modeling of Weld Bead Geometry, Quality and Productivity for Stainless Steel Claddings Deposited by FCAW, Journal of Materials Engineering and Performance, 2011, 21: 1862-1872.
10. Yunus A. Cengel, Introduction to Thermodynamics and Heat Transfer, Second Edition, The McGraw-Hill companies, 2008.
11. Holman. J. P., Heat Transfer, 9th ed., Tata McGraw-Hill publishing company Limited, New Delhi, (2008).
12. Kothandaraman. C. P., Subramanyan. S., Heat and Mass transfer data book, Eighth edition, New Age International Publishers, 2014.
13. Siva K, Murugan N, Raghupathy VP. Modelling, analysis and optimisation of weld bead parameters of nickel based overlay deposited by plasma transferred arc surfacing. Archives of Computational Materials Science and Surface Engineering, 2009, 1(3):174-82.
14. Murugan N, Gunaraj V. Prediction and control of weld bead geometry and shape relationships in submerged arc welding of pipes. Journal of Materials Processing Technology, 2005, 168(3):478-87.
15. Parmer. R. S., Welding Processes and Technology, Khanna Publishers, New Delhi, (1992).
16. Jhavar S, Jain NK, Paul CP. Enhancement of deposition quality in micro-plasma transferred arc deposition process. Materials and Manufacturing Processes, 2014, 29(8):1017-23.
17. Benyounis KY, Olabi AG. Optimization of different welding processes using statistical and numerical approaches–A reference guide. Advances in engineering software, 2008, 39(6):483-96.

*****